ISBN: 978-3-95450-240-0 ISSN: 2673-5539 doi:10.18429/JACoW-RuPAC2021-WEPSC20

MAGNETS DESIGN FOR 2.5 GeV BOOSTER SYNCHROTRON

A.S. Smygacheva, V.N. Korchuganov, Ye.A. Fomin
NRC «Kurchatov Institute», Moscow, Russia

Abstract

The Project of complete modernization of the current accelerator complex is in progress in the NRC «Kurchatov Institute». The development of a new booster synchrotron as a part of the injection complex for a new 3-d generation synchrotron light source is included in the Project. The booster synchrotron has 24 dipoles, 60 quadrupoles, 48 sextupoles and 24 correctors. In order to obtain the required field quality, 2D- and 3D-simulations of magnets were carried out. The obtained geometry for each of the magnets is presented in the paper.

INTRODUCTION

The booster synchrotron is based on the modified DBA structure with 12 cells, each with mirror symmetry about the center of the cell [1]. One cell consists of 2 dipoles, 5 quadrupoles, 4 sextupoles and 2 correctors. The booster lattice has a large dynamic aperture with compensated natural chromaticity and low natural emittance (43.4 nm×rad). The structure is stable against various kinds of magnetic field errors within the permissible values.

The sensitivity of the booster lattice to errors and the parameters of the electron beam set the requirements for the quality of the magnetic fields. Optimization of the main characteristics of the field (the integral homogeneity of the field and the effective length) to the required values is carried out by searching the magnet pole geometry in 2D- and 3D-simulations of magnetic fields. The manufacturing technology and the magnetic properties of the steel have to be taken into account during magnet field optimization.

The booster synchrotron will operate in a cyclic mode with a frequency of 1 Hz in the energy range from 200 MeV to 2.5 GeV. The presence of alternating magnetic fields determines the manufacturing technology of the magnets of the booster synchrotron. The yoke of each magnet will be laminated, i.e. will be assembled from 1 mm thick magnetic steel sheets. The steel chosen for the magnet yokes is M940-100A. To ensure high quality of the magnetic field, the profile of each sheet must be made with an accuracy of 10–20 µm. The entire internal geometry of the magnet yoke must be maintained with the same accuracy during assembly.

The paper presents the optimization results of magnetic fields, electrical parameters and geometry of the booster magnets. 2D- and 3D-simulations of magnetic fields were carried out in the CST Studio Suite [2].

DIPOLES

The dipole magnet is a sector bending magnet. The ends of the magnet are parallel to each other. The main dipole parameters are presented in Table 1. The cross section of the dipole is shown in the Fig. 1.

The dipole magnet has also two additional coils for the field correction. The cross-sectional conductor size is 3.15×3.15 mm^2. The maximum current is 10 A in the correction coils.

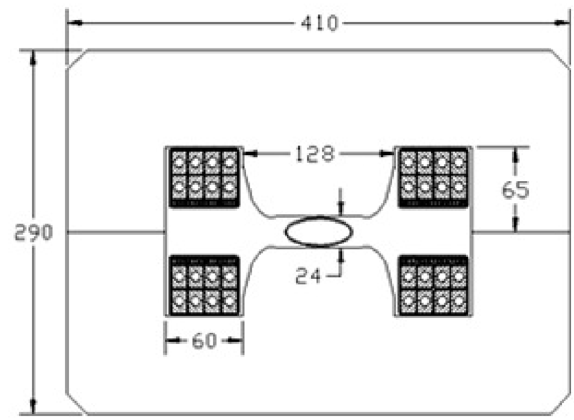

Figure 1: The dipole cross section.

Table 1: Dipole Parameters

Number of magnets	24
Deflection angle, deg	15
Magnetic field, T	0.1-1.3
Magnetic length, mm	1679.363
Yoke length, mm	1674
Curvature radius, mm	6415
Gap, mm	±12
Homogeneity within the GFR	$\leq \pm 2\times10^{-4}$
Number of coils	2
Number of turns per pole	8
Conductor cross section/ Inner hole diameter, mm^2/mm	18×12/ 8
Max. current, kA	1.56
Resistance per magnet, mΩ	6.47
Inductance per magnet, mH	2.86
Max. power loss, W	15.8
Pressure drop, bar	4
Cooling water flow rate, l/min	17.3
Temperature rise, °C	13.1
Magnet weight, kg	1500

The geometry of the pole, obtained in 2D- and 3D-simulations, provides the dipole field homogeneity in the central section of the magnet better than $\pm 5\times10^{-5}$ in a good field region (GFR) of 20×40 mm^2 (h×w) and the integral homogeneity of $\pm 2\times10^{-4}$ (Fig. 2). To reduce the

Content from this work may be used under the terms of the CC BY 4.0 licence (© 2021). Any distribution of this work must maintain attribution to the author(s), title of the work, publisher, and DOI

ISBN: 978-3-95450-240-0 ISSN: 2673-5539 doi:10.18429/JACoW-RuPAC2021-WEPSC20

magnetic saturation effect in the pole the Rogowski curve [3] was used for forming the transverse profile. To reduce distortions of the dipole field homogeneity in the GFR with increasing energy, the transverse profile has symmetrical shims directed to the horizontal plane of symmetry of the magnet. The magnet pole ends are formed by three planes to make the integral homogeneity symmetrical in the horizontal direction.

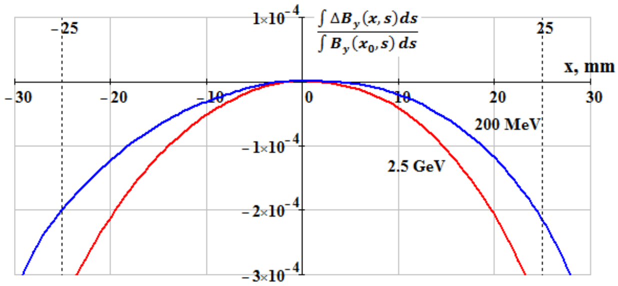

Figure 2: Integral homogeneity of the dipole field.

QUADRUPOLES

The quadrupole magnets of the booster synchrotron are grouped into three families: two families of focusing lenses and one family of defocusing lenses. The main quadrupoles parameters are presented in Table 2. The cross section of the quadrupole is shown in the Fig. 3.

The quadrupole magnet has also the 4 additional coils for field gradient correction. The cross-sectional conductor size is 3.15×3.15 mm^2 for additional coil. The maximum current is 9.3 A.

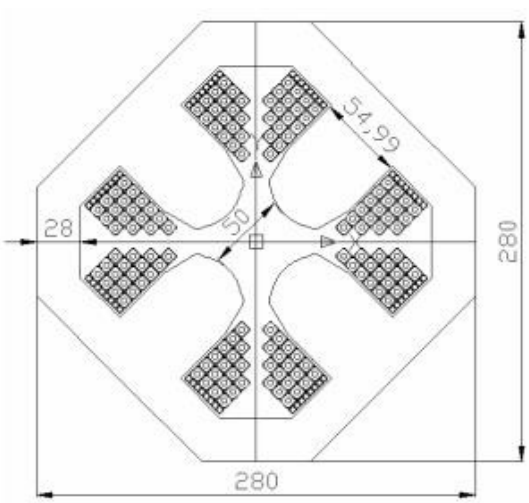

Figure 3: The quadrupole cross section.

The hyperbolic shape of the poles allows maintaining the constancy of the gradient of the quadrupole field in the working area of the magnet. Note, due to the magnetic saturation effect the effective length of the magnet differs at different energy levels. In addition, with the increasing current in the coils nonlinearities of the effective length and the field gradient arise. It is important to keep the product of these quantities at a high energy level (at 2.5 GeV).

The searched geometry of the magnet pole provides the homogeneity of the magnetic field gradient in the central section of the magnet better than ±1×10^{-4} in the GFR and the integral inhomogeneity better than ±5×10^{-4} (Fig. 4). The geometry of the pole ends was chosen so that the effective length is 320 mm at energy of 2.5 GeV.

Table 2: Quadrupole Parameters

Quadrupole magnets	Q1	Q2	Q3
Number of magnets	24	24	12
Max. gradient (2.5 GeV), T/m	21.12	-23.55	20.89
Magnetic length, mm	320		
Yoke length, mm	300		
Homogeneity of gradient within the GFR	$\leq \pm5\times10^{-4}$		
Number of coils	4		
Number of turns per pole	18		
Conductor cross section/ Inner hole diameter, mm^2/mm	7×7/ 3.5		
Current at max. gradient, A	292	325	289
Resistance per magnet, mΩ	26		
Inductance per magnet, mH	4.3		
Max. power loss, kW	2.22	2.75	2.17
Pressure drop, bar	4		
Cooling water flow, l/min	5.7		
Water temperature rise, °C	6.6	9.28	8
Bore radius, mm	25		
Magnet weight, kg	70		

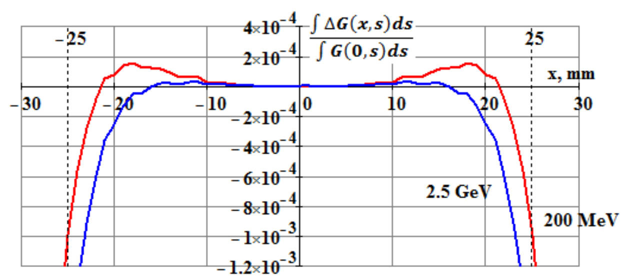

Figure 4: Integral homogeneity of the quadrupole field gradient.

SEXTUPOLES

The main sextupoles parameters are presented in Table 3. The cross section of the sextupole is shown in the Fig. 5.

The geometry of the transverse pole profile is set by a parabola, since the sextupole magnet provides a quadratic growth of the magnetic induction with radius. The pole ends are formed by one plane. The searched pole geometry provides an integral homogeneity of ±1×10^{-3} in the energy range 200 MeV to 2.5 GeV in the GFR (Fig. 6). This value is achieved with an increased homogeneity in the central section: the homogeneity changes in the range from 0 to +2.3×10^{-3} in the GFR at energy of 200

Content from this work may be used under the terms of the CC BY 4.0 licence (© 2021). Any distribution of this work must maintain attribution to the author(s), title of the work, publisher, and DOI

ISBN: 978-3-95450-240-0 ISSN: 2673-5539 doi:10.18429/JACoW-RuPAC2021-WEPSC20

MeV and in the range from 0 to $+1.7\times10^{-3}$ at energy of 2.5 GeV.

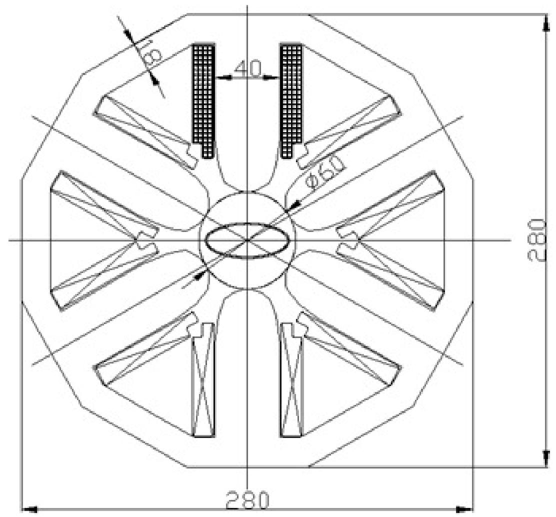

Figure 5: The sextupole cross section.

Table 3: Sextupole Parameters

Sextupole magnets	SD	SF
Number of magnets	24	
Max. sextupole gradient (2.5 GeV), T/m^2	-215	90
Magnetic length, mm	100	
Yoke length, mm	100	
Homogeneity of sextupole gradient within the GFR	$\le\pm1\times10^{-3}$	
Bore radius, mm	30	
Number of coils	6	
Number of turns per pole	86	
Conductor cross section, mm^2	2.5×2.5	
Current at max. gradient, A	9	3.7
Resistance per magnet, mΩ	397	
Inductance per magnet, mH	66.9	
Max. power loss, W	32.2	5.6
Magnet weight, kg	25	

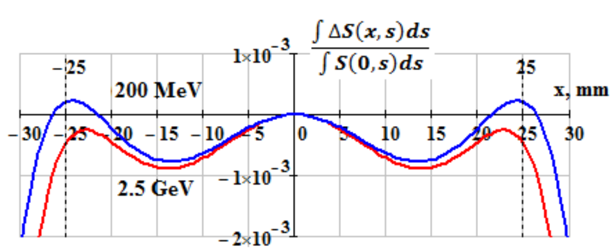

Figure 6: Integral homogeneity of the sextupole field.

CORRECTORS

The correcting magnet combines the functions of a horizontal and vertical corrector and is a frame dipole magnet (Fig. 7). The corrector provides a maximum angle of rotation of the particle trajectory of 0.48 mrad with a magnet yoke length of 100 mm. The effective length is 200 mm.

The corrector has the 4 main excitation coils. The cross-sectional conductor size is 2×2 mm^2. The maximum current is 7.2 A in the coils. The number of turns per coil is 266.

The integral homogeneity of the field is 2×10^{-2} in the GFR (Fig. 8). The sextupole component of the field is 1.78 T/m^2, which is less than the field value in the sextupole.

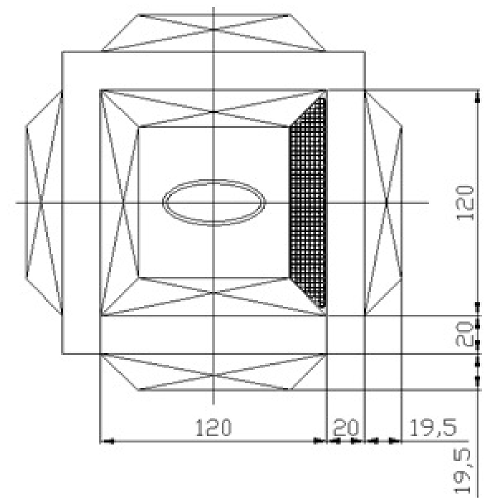

Figure 7: The corrector cross section.

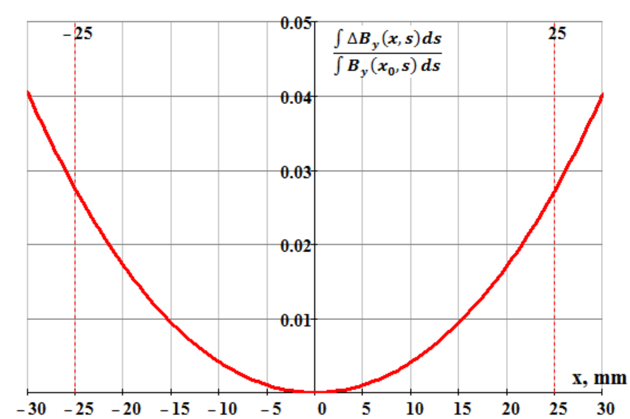

Figure 8: Integral homogeneity of the corrector field.

CONCLUSION

The geometry of each type of magnetic elements of the booster synchrotron is optimized in order to obtain the required parameters and quality of the magnetic field. However, we are considering the possibility of replacing the coils and small changes in the geometry of the dipole magnet due to the dense arrangement of the elements on the ring of the booster synchrotron. Also note, after the prototype is made and the magnetic measurements are carried out the geometry of the poles of each type of magnet can be corrected to achieve the required parameters of the magnetic field.

Content from this work may be used under the terms of the CC BY 4.0 licence (© 2021). Any distribution of this work must maintain attribution to the author(s), title of the work, publisher, and DOI

ISBN: 978-3-95450-240-0 ISSN: 2673-5539 doi:10.18429/JACoW-RuPAC2021-WEPSC20

REFERENCES

[1] A.S. Smygacheva, V.N. Korchuganov, and Ye.A. Fomin, "2.5 GeV booster synchrotron for a new Kurchatov synchrotron radiation source", presented at RuPAC'21, Crimea, Russia, Sep. 2021, paper TUPSB33, this conference.

[2] CST Studio Suite, `http://www.3ds.com`

[3] W. Rogowski, "Die elektrische Festigkeit am Rande des Plattenkondensators", Archiv f. Elektrotechnik, vol. 12, March 1923, pp. 1-15, `https://doi.org/10.1007/BF01656573`

© Content from this work may be used under the terms of the CC BY 4.0 licence (© 2021). Any distribution of this work must maintain attribution to the author(s), title of the work, publisher, and DOI